

## **Nondimensional convection numbers modeling thermally stratified storage tanks: Richardson's number and hot-water tanks**

Joseph, Rendall<sup>a,b\*</sup>, Ahmad, Abu-Heiba<sup>a</sup>, Kyle, Gluesenkamp<sup>a</sup>, Kashif, Nawaz<sup>a</sup>, William, Worek<sup>b,c</sup>, Ahmed, Elatar<sup>a</sup>

<sup>a</sup>Building and Transportation Science Division, Oak Ridge National Laboratory, Oak Ridge, TN, USA

<sup>b</sup>Texas A&M University – Kingsville National Laboratory, Kingsville, TX, USA

<sup>c</sup>Argonne National Laboratory, Lemont, IL, USA

\*Corresponding author

[rendalljd@ornl.gov](mailto:rendalljd@ornl.gov)

### **ABSTRACT**

Thermally stratified storage tank studies have spanned over 50 years to increase the thermal storage efficiency and accurate prediction of the outlet temperature particularly for solar applications. The studies have reviewed and modeled the jet and plume flow phenomena inside the tank due to the inlet mixing and stratification level. Kelvin–Helmholtz and Rayleigh–Taylor instabilities are the major drivers of the mixing in these tanks. Momentum jets deflecting off walls at the bottom of the tank also create significant mixing. Reviewing Richardson models shows that the categorization was based on the range of Reynolds numbers at the inlet. Unfortunately, the use of superficial velocity in calculating the Richardson number results in critical values in the literature ranging from below 0.25 to 100. The most used length scale associated with these flows is an inertial scale based on the tank height or diameter although the mixing can occur at a relatively smaller scale. The various inlet devices and a large span of flow rates experienced in thermally stratified storage tanks requisite the use of the Reynolds number in combination with a convection number for accurate one dimensional models for prediction of performance over long-term. The evaluation of peak shifting of electric loads leveraging from renewable sources for applications including residential hot-water tanks, commercial water tanks, and large-scale chilled water storage tanks require such models. This paper is focused on establishing the significance of the convection numbers in conjunction with the Reynolds number for modeling the thermal stratification in storage tanks.

Word count:10,438

Keywords: solar thermal energy storage, Richardson number, Reynolds number

### **Highlights**

- Reynolds and Richardson numbers characterize mixing in thermally stratified storage tanks.
- The Richardson number is related to other convection-based nondimensional numbers.
- The Richardson number has been inconsistently used in tank modeling.
- At Reynolds number  $< 3,300$ , many correlations exist in the literature.
- Reynolds and Richardson relationship is robust over a range Reynolds number's.

This manuscript has been authored in part by UT-Battelle, LLC, under contract DE-AC05-00OR22725 with the US Department of Energy (DOE). The US government retains and the publisher, by accepting the article for publication, acknowledges that the US government retains a nonexclusive, paid-up, irrevocable, worldwide license to publish or reproduce the published form of this manuscript, or allow others to do so, for US government purposes. DOE will provide public access to these results of federally sponsored research in accordance with the DOE Public Access Plan (<http://energy.gov/downloads/doe-public-access-plan>).

## Nomenclature

$A$	cross-sectional area ( $m^2$ ) or Atwood number
$Ar$	Archimedes number
$AR$	aspect ratio
$Bi$	Biot number
$D$	diameter of a tank (m)
$C$	Courant number
$C_p$	specific heat at constant pressure (W/kg K)
$EDF$	Eddy conductivity factor
$Fr$	Froude number
$g$	gravity ( $m/s^2$ )
$Gr$	Grashof number
$Gr(I)$	stratification gradient number
$H$	vertical distance (m)
$\Delta h$	local height difference (m)
$Jo$	buoyancy flux ( $m^4/s^3$ )
$k$	thermal conductivity (W/m K)
$L$	length scale (m)
$M_o$	momentum flux ( $m^4/s^2$ )
$N$	wave number or Kelvin-Helmholtz frequency
$P$	perimeter (m)
$Pe$	Peclet number
$S$	shear rate (1/s)
$Str$	stratification number
$Ra$	Rayleigh number
$Ri$	Richardson number
$Re$	Reynolds number
$T$	temperature ( $^{\circ}C$ )
$u_a$	horizontal cross-flow velocity (m/s)
$U$	horizontal average velocity (m/s)
$v$	velocity in the vertical direction (m/s)
$\dot{V}$	volumetric flow rate ( $m^3/s$ )
$V$	superficial velocity, perpendicular to thermocline (m/s)
$y$	height in vertical direction (m)
<b>Greek</b>	
$\alpha$	thermal diffusivity ( $m^2/s$ )
$\varepsilon_d$	dissipation rate of turbulence ( $m^3$ )
$\varepsilon_H$	eddy conductivity ( $m^2/s$ )
$\rho$	Density ( $kg/m^3$ )
$\rho_{\bar{T}}$	density at the weighted average temperature ( $kg/m^3$ )
$\rho'$	reduced density $\Delta\rho/\rho_{ref}$
$\partial\bar{\rho}/\partial y$	average density gradient ( $kg/m^4$ )
$\nu$	kinematic viscosity ( $m^2/s$ )
<b>Subscripts</b>	
$c$	critical
$C$	cold temperature
$H$	hot temperature or thermal eddy
$o$	reference density
$m$	mean
$st$	strict and gradient definition of $Ri$
$sf$	superficial velocity used for calculation of $Ri$
$tank$	horizontal cross-sectional area of the tank

## 1. Introduction

The most critical component in the thermal stratification model of hot-water tanks is predicting the temperature of water delivered to the user for their hot-water needs. In hot-water systems for domestic use, delivery temperatures need to be hot enough to satisfy disinfection requirements, and cold enough to prevent scalding. Furthermore, thermally stratified storage tanks (TSSTs) in residential and commercial buildings are of growing interest for peak-shifting the electrical demand associated with hot-water loads. The control of the hot-water tank by utilities will increase the dynamics seen in hot-water tanks, and accurate modeling of the outlet temperature is critical.

TSSTs typically have a region with a large thermal gradient present due to complex natural convection heating and gravity forces; this region is called the “thermocline.” The thermocline can reduce mixing in the upper portion of the tank, keeping the water delivery temperature higher than in a fully mixed tank. As a TSST is discharging, the incoming water, which is initially a momentum jet, can deflect off tank walls and form negatively buoyant plumes that interact with the thermocline region through Kelvin [1]–Helmholtz [2] (KH) instabilities. When a TSST is recharged by an external heat source, the hot water entering the top of the tank also creates a negatively buoyant jet that causes Rayleigh [3]–Taylor [4] (RT) instabilities and sometimes also causes KH instabilities. “Entrainment mixing” is a phrase used in the literature to describe mixing when KH and RT instabilities are not readily identified, or it describes the combination of the instabilities. Correctly identifying the phenomenon is the first step to modeling a system, and much progress has been made in the area of TSSTs.

Historically, mixed tank models, stratified tank models, and jet-entrainment models were developed to simulate this complex behavior in TSSTs with varying success. Two recent papers that quantify the success of modeling TSSTs include a sensitivity paper by Arias et al. for long-term studies [5] and a review by Chandra and Matuska [6]. The review showed approaches to modeling TSSTs that linearize the thermocline region with different numerical methods and these approaches are appropriate in for linear thermoclines – which is often not the case. Empirical factors are used to improve model accuracy as in the case of two calibration coefficient studies. Shen et al. calibrated section-wise in the tank energy balance [7]. Ref. [8] used nonsmoothed functions were represented by a log-sum-exp function and scaling factor. Empirical factors, often associated with nondimensional numbers, extend the applicability of the model to different of inlet diffusers, inlet velocities, and properties of the fluid in the tank, whereas the previously mentioned empirical factors can be applied for only a small range of values. These references to nondimensional numbers and models will be the focus of this paper. This review supports the findings of Oppel et al. [9] and Zurigat et al. [10] that the Reynolds ( $Re$ ) and Richardson ( $Ri$ ) numbers are most appropriate for modeling TSSTs. Recent studies in computational fluid dynamics (CFD) and exergy analysis will be briefly overviewed before diving into 1D nondimensional number modeling approaches.

Many CFD models have been created to study stratification in hot-water tanks. A novel design with a down-spout inlet and heater at the bottom of a tank was studied by Abdelhak et al. [11] in which the mixing zone had a random mesh, and above the heater, a rectilinear mesh was used that matched the experimental results well. The impact of aspect ratio was examined by a CFD model and the resulted confirmed the aspect ratio ranging from 3 to 4 as optimal [12]. Stratification that occurs from heat loss at the walls of the tank was studied and quantified by Fan and Furbo [13]. The hydrodynamic flow in a wrapped heat pump water heater was modeled for typical domestic hot water flow rates by Elatar et al. [14]. The impact of internal structures on stratification was examined using a CFD model by Li et al. [15]. Shi et al. studied the effect of the use pattern on a heat pump water heater in a CFD model [16]. A rectangular tank was studied by CFD by Kaloudis et al. with a large eddy simulation turbulence model that incorporated gravity currents and reverse flow along the bottom of a rectangular tank [17]—all these CFD models use K-epsilon turbulence modeling.

Exergy-based methods of modeling TSSTs have also been applied by many authors and although not the focus of this paper, a few papers are of note. Along with creating a CFD model, Bai et al. studied the entropy production rate and exergy efficiency of the tank and found that an aspect ratio of 1 gave the highest

efficiency, but an aspect ratio greater than 3 had little influence on the stratification [18]. Kalouis et al. also included exergy analysis in their study of a rectangular tank and found slot diffusers to create less entropy than circular diffusers common in hot-water tanks. The exergy generation of a novel diffuser that redistributed the flow from a circular diffuser to a larger circumference showed that the fastest and slowest charge rates (6 and 1 L/min, respectively) had the lowest exergy efficiency over time [19]. A system exergy model was created for air-source water heating heat pumps by Ju et al. [20]. The stratification in a phase change material (PCM) heat exchanger was studied by Wu et al. [21] in which the temperature difference between the PCM and the water was the largest contribution to exergy production. A CFD simulation that included exergy analysis of experimental data showed good agreement by Wang et al. [22]. In a novel design of floating PCM spheres, the exergy analysis showed the highest exergy efficiency with a PCM temperature near the hottest temperature where the spheres were located near the bottom of the tank [23]. Charging exergy performance was studied by Njoku et al. in which the  $Ri$  number and aspect ratio were found to have little impact on exergy generation, but the Peclet number ( $Pe$ ) had a significant impact [24]. Lake and Rezaie studied the exergy efficiencies in cold-water storage in four tank sections where the charging and discharging exergy efficiency were calculated. They found that the basic models greatly overestimated the exergy efficiency of charging for their system and underestimated the exergy efficiency of discharging [25].

New research in the area of stratified tanks shows ongoing attempts to characterize the tanks. Many methods have been used to model the mixing dynamics in hot-water tanks, including empirical factors for mass flow [26] and calibration factors for heat transfer [7]. The interactions have been modeled by 3D CFD with limited success over a wide range of inlet  $Re$  numbers. Bai et al. studied a cylinder tank in which the heat loss over long periods of time was studied, and they determined correlations for the centerline temperature through experimentation and CFD [27]. Zhang et al. suggested a spatial temperature uniformity coefficient to define the performance of the stratified tank [28]. Chandra and Matuska [29] studied  $Ri$  number values between 0.6 to 110 and inlet  $Re$  number values up to 6,440 for horizontal inlet devices [29]. Stratification due to additional components in TSSTs has also been studied [30]. The use of neutrally buoyant spheres full of PCM and the impact on the thermocline was quantified by Ref. [22]. Shen et al. [7] studied a condenser coil on the outside of the tank, and Baeten et al. [30] modeled a condenser coil on the inside of the tank. Both these studies found that stratification is important to the performance of the heat pump. In a solar thermal system, Jadhav et al. reported the capital investment can reduce by 28% when stratification is maintained [31].

In this paper, we review nine nondimensional numbers that have been used to model stratified tanks, focusing on the convection- or mixing-based nondimensional numbers, specifically focusing on the  $Ri$  number. The  $Ri$  number has been used in oceanic studies to characterize mixing and predict whether bulk mixing will occur [32]. Jordan and Furbo found  $Ri$  could also characterize mixing in small solar domestic storage tanks [33]. Furthermore, nondimensional numbers, such as  $Ri$  and  $Re$ , quantify the phenomena of physics-based interactions with a few inputs such as property-based information about the fluid and information about the flow regime of the bulk fluid and surface temperature of solid bodies in interaction with the fluid. In the case of stratified tanks, it is important to capture the temperature range of the thermocline, the viscosity, and the inlet velocity (and direction) of the inlet fluid in the nondimensional numbers that are used to model TSSTs.

## 2. Mixing phenomena

Before describing the dynamics of mixing phenomena inside a tank, a quiescent tank will be briefly described. A tank full of water left in an ambient environment will eventually approach a uniform temperature because of conduction through the water and convection in the tank due to heat lost to the ambient environment. The losses to the ambient convection through the tank walls typically decreases the strength of the thermocline [13]. In some cases, the thermocline increases in thickness without significantly decreasing the overall temperature difference between the hottest and coldest parts of the

tank when the heat loss is minimized and the ambient temperature of the storage matches a temperature in the thermocline [18]. These convection and conduction effects occur on a long time scale.

The dynamics during a cold-water draw create significant RT and KH mixing on a short time scale. RT mixing is due to gravitational accelerations for a cold-heavier fluid through lighter fluid or a hot-lighter fluid through a heavier fluid—these can be considered a vertical mixing phenomenon for TSSTs. KH mixing is due to internal waves between layers of stratification. Waves that break when colliding with the tank wall can be considered entrainment (ET). ET can also be a combination of KH and RT mixing. These three types of mixing, on a short-time scale, are the mixing phenomena during inlet and outlet flows of a TSST.

During the water draw from the tank (discharge), the cold water entering the tank through the inlet device is often a momentum jet with significantly higher velocity than the bulk flow of water in the tank. This higher-velocity water traveling through the bulk water in the tank creates entrainment mixing (ET Figure 1). The layering of similar density water also creates internal waves (KH1 Figure 1). Horizontal jets from vertical inlet devices with perforations also create internal waves (enlargement Figure 1). Contact with the bottom of the tank will also cause buckling when the density of the incoming fluid is different from that of the storage (enlargement Figure 1) [34]. In the literature reviewed, only Cole and Bellinger mentioned that dip-tubes (vertical tube inlets - VTI) reduce thermal stratification [35].

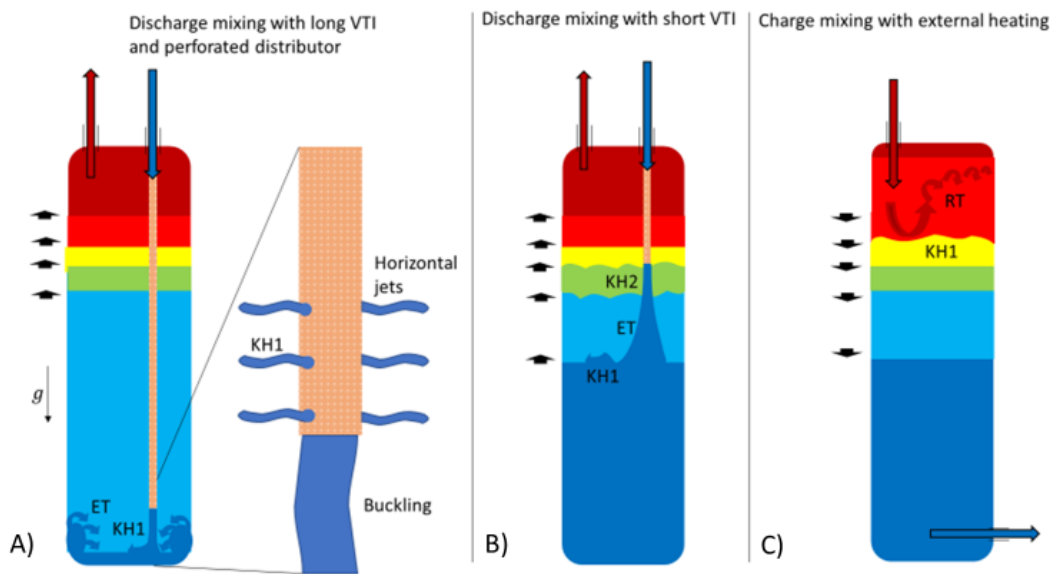


Figure 1 Mixing in TSSTs due to RT or KH instabilities and entrainment mixing (ET) for vertical inlets when (A) delivering cold water below the thermocline, (B) delivering water in the thermocline region, and (C) delivering hot water above the thermocline.

The instability within the fluid is the root cause for turbulence generation [36]. The instability generated in fluids is mainly due to buoyancy forces, instability, and/or fluctuations in shear flow [36]. The fluid characteristics inside TSSTs suggest the potential generation of turbulence due to any of the aforementioned sources, as well as turbulence from the inlet device. During charging and discharging, instability between the shear layers is possible. On the other hand, the heating process inside the tank generates buoyancy driven currents, which can lead to instability and turbulence in the fluid (not pictured because there are multiple heating designs). The importance of the instability characteristic inside TSSTs relates to local mixing, which is most significant in the bottom of the tank. The fluid inside most of the tank will have distinct characteristics in the mean flow domain, which has a large length scale, and the turbulent flow domain, which is associated with small length scales (either at the tank inlet/outlet or internal/external

heaters). In the mean flow domain, vortices and convective cells are formed and can be easily identified during the heating process. These characteristics contribute to mixing. The fluctuating/turbulent flow domain includes vortices, which can contribute to mixing. The length scale in the turbulent flow field plays a significant role in the vortices dynamics and dictates the flow energy transfer at these length scales. If the length scale is larger than Taylor microscale, the viscosity has minor effects on vortices. Taylor microscale is the intermediate length scale at which fluid viscosity significantly affects the dynamics of turbulent eddies [36]. If the length scale is smaller than Taylor microscale, flow viscosity dominates turbulence motion and works on dissipating the kinetic energy into heat. Therefore, turbulent characterization is recommended in TSSTs to understand the physical processes that might occur and have noticeable effects. Elatar et al. [14] conducted a detailed investigation on fluid mean and turbulent behavior inside TSSTs and found the turbulence kinetic energy production in the lower (inlet) region is  $0.9 \text{ m}^2/\text{S}^3$ , the middle (stratified) region is around  $0.2 \text{ m}^2/\text{S}^3$ , and the upper (outlet) region is around  $0.5 \text{ m}^2/\text{S}^3$  for discharges.

Furthermore, momentum jets can also trigger KH instability when water is directed vertically through a thermocline by a short vertical tube inlet and create waves along the stratified region like a rock dropped in water (KH2 Figure 1). Waves created by momentum jets can deflect off the tank walls and at the right wavelength may amplify and cause large scale mixing. KH1 instabilities in Figure 1 are easier to measure than KH2 because KH2 can appear as noise in the temperature measurement. Similarly, RT instabilities in Figure 1 and Figure 2 can be seen as temporarily hotter or colder recordings of temperature.

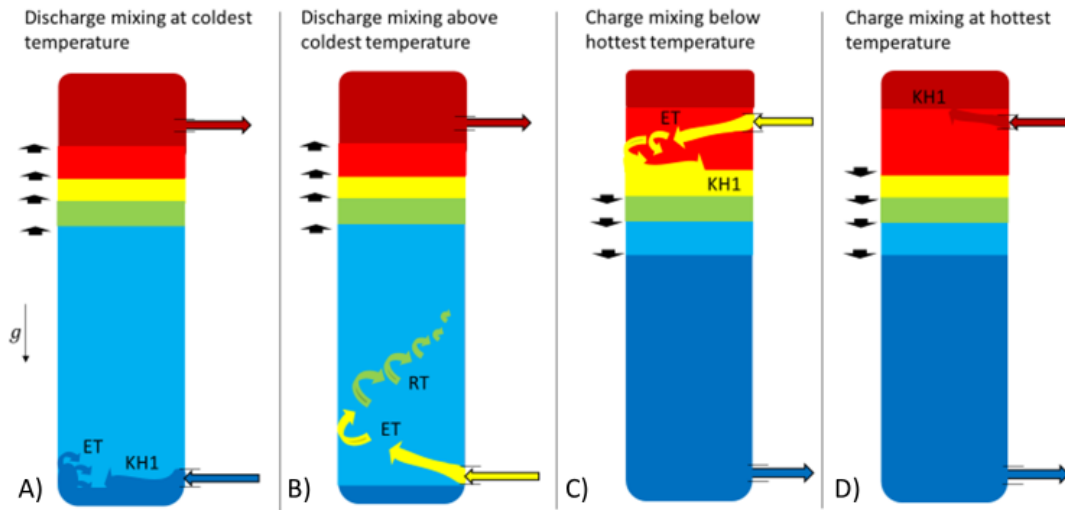


Figure 2 Horizontal inlet mixing in TSSTs due to RT or KH instabilities and entrainment mixing (ET) for vertical inlets when (A) delivering cold water below the thermocline, (B) delivering warm water below the thermocline region, (C) delivering warm water above the thermocline, and (D) delivering hot water in the thermocline region.

The phenomena in Figure 1 are shown when the discharge and charge temperatures are equal to the coldest and hottest temperature in the tank, respectively, which is not always the case. The effect of gravity (inlet jet curving up or down) on the inlet jet is secondary to the momentum at higher velocities, and the impact is more clearly shown in the cases of horizontal inlets in Figure 2. As the inlet jet carries higher horizontal velocity, the KH1 instabilities are greater in the case of horizontal inlets. The type of mixing and the level of mixing in the cases shown in Figure 1 and Figure 2 depend on geometry, temperatures, and velocities.

The first type of KH instability (KH1) is due to horizontal velocity difference between the inlet water and tank water. This velocity difference can occur directly in the case of horizontal inlet (not shown), or after deflection against walls in the case of vertical inlets. Vertical inlet devices with horizontal jets create KH instability and bulk mixing directly. This type of bulk mixing is most noticeable in the first couple of seconds of a draw as a measurable difference in the temperature between the inlet and the coldest portion

of the tank. This temperature difference is carried throughout long draws because the temperature at the bottom of a TSST is always warmer than the cold inlet temperature.

Under the right circumstances, the major instabilities in TSSTs during a draw can be localized and a thermocline can be created by the inflowing water. The creation of a thermocline in TSSTs takes place when the momentum in the inlet jet has been dissipated, the major KH mixing is complete, and similar temperature fluid is arranged in a layer by gravity forces. A thermocline will be created in either hot water entering the top of the tank or cold water entering near the bottom of the tank when adequate conditions are present. These conditions are described by the critical  $Ri$  number ( $Ri_c$ ) as  $Ri$  is ratio of the buoyancy forces to the shearing velocity in stratified flows. Bulk mixing ceases when the buoyancy forces are larger than the shearing forces and the  $Ri_c$  for stratified flows is  $Ri = 0.25$  as found in oceanic studies [32]. The optimal mixing was studied by Camassa et al., who showed that stable and sharp or step-wise thermoclines were the most efficient. They also characterized the effect of walls on negatively buoyant plumes [37]. Park, et al. showed that the  $Re$  number of a rod vibrating in a stratified tank was also critical to mixing characterized by the  $Ri$  number [38]. The turbulence level of the incoming cold fluid in a vertical tube inlet was correlated by the authors in another paper to  $Re/Ri$  [39].

Without describing the initial bulk mixing in a tank, models that assume full tank mixing initially underpredict the outlet temperature and as they progress in time, overpredict the outlet temperature. Some other models describe the thermocline as the linear temperature difference between the hot- and cold-water temperatures. These models overpredict the outlet temperature when the thermocline is too close to the bottom of the tank and a large flow rate of hot water is demanded. To compensate for these discrepancies, correction factors are applied to the inlet, the outlet, or both to account for the major type of instabilities under at least one tank flowrate. Models that have inlet and outlet mixing efficiencies that are not based on flow velocities will not describe the thermocline thickness at high or low flow rates. A high flow rate case creates bulk mixing in a larger quantity than predicted, and a low flow rate case can create two thermoclines in a tank [40]. These complexities are often not represented in simple models [41]. The  $Re/Ri$  relationship can be applied as a function of height and add to thermal diffusivity in the conduction equation based on the flow rate of the inlet fluid to capture the complex dynamics in the bottom and top of the tank

Although  $Re/Ri$  was determined to adequately describe turbulent inlets in the early 1990s, many other numbers have been used before and after this discovery for laminar cases, uninsulated tanks, and so on. The nondimensional numbers used to characterize the stratified tanks are based on the convection or advection, conduction, quiescent (initially stagnate) fluid, geometry, and efficiency of TSSTs. Describing the convective flow in a TSST involves combining fast dynamics in the inlet mixing zone and slow dynamics of the bulk flow. The complexity of a model using  $Ri$  and  $Re$  compared with models that consider conduction is minimal because the second derivative of temperature with regard to height is already in the model [9].

To model the convective mixing in one dimension with nondimensional numbers, authors typically use the  $Re$  number,  $Ri$  number, Froude number ( $Fr$ ), Grashof number ( $Gr$ ), Rayleigh number ( $Ra$ ), or  $Pe$  number. Ten nondimensional numbers will be reviewed in the next sections, with eight being convection-based and two quiescent fluid-based numbers used to model TSSTs.

### 3. Convection numbers

Convection-based nondimensional numbers characterize the heat transfer of a moving fluid with another surface or fluid. For modeling convection in hot-water tanks, different nondimensional numbers can be chosen in which some are mathematically related to the  $Gr$  number,  $Ri$  number, and  $Fr$  number. All three numbers will be discussed in this section, plus a few others, but the flow-based  $Re$  must be addressed first. A full list nondimensional numbers reviewed for TSSTs is shown in **Table 1**.

Table 1 Dimensionless groupings used in literature and their definitions.

Dimensionless number	Relationship	Reference(s)	Article's	Remarks
Convection-based				
Archimedes	External forces	[33], [42]	2	Similar to the Richardson number and successfully used in purely laminar cases
	Internal viscous forces			
Biot	Fluid surface convection	[25], [43], [44]	3	Typically used for uninsulated tanks or tanks with high conductivity fluids (i.e., thermal oils)
	Conductivity of solid			
Froude	Inertial forces	[45]–[51]	7	Mathematically related to the Richardson number and only smaller in scale
	Gravitational forces			
Grashof	Buoyancy force	[25], [52]–[56]	6	Typically used to quantify heat loss on the walls of the tank or as an intermediate step to calculating the Richardson number for stratification analysis
	Viscous force			
Peclet	Heat transfer convection	[17], [24], [42], [57]–[62]	9	Used when the fluid has a high thermal conduction or for diffusion of chemical species (e.g., salt)
	Heat transfer conduction			
Rayleigh	Thermal diffusion	[17], [63], [64]	2	Criteria to determine laminar flow or critical value for mixing using a characteristic length (e.g., 1 cm [63])
	Thermal convection			
Reynolds < 3,300	Inertial force	[9], [17], [39], [44], [49], [50], [55], [58], [60], [65]–[78]	22	Describes the bulk flow within the tank
Reynolds > 3,300	Viscous force	[14], [33], [42], [45], [73], [76], [79]	7	Describes turbulence in the inlet device
Richardson	Buoyancy force	[9], [10], [14], [34], [46], [62], [68], [78], [80]–[86]	15	Stability of stratification in TSSTs based on buoyancy flows within the tank
	Momentum			
Quiescent fluid-based				
Atwood	Fluid density difference	[49], [87]	2	Used to identify the strength of the thermocline based on density difference
	Sum of fluid densities			
Stratification	Local thermal gradient	[13], [49], [88], [89]	4	Used to identify the strength of the thermocline based on temperature difference
	Total thermal gradient			

### 3.1 Reynolds number

$Re$  characterizes if the flow is turbulent or laminar. A round jet is turbulent at a  $Re$  greater than around 200 [78]. Although 200 is the applicable definition for turbulence from an inlet device, it is almost always exceeded in the domestic use of TSSTs [40].  $Re$  values in vertical-tube inlets are often greater than 5,000 (~1 GPM) through a  $\frac{3}{4}$  in. tube; sometimes,  $Re$  values reach 40,000 (~3 GPM) for small-diameter tubes ( $\frac{5}{8}$  in.) and therefore, turbulent inlet models should be at least used for the inlet area.

For the piping or tube before an inlet, the flow regime is laminar flow for  $Re$  below approximately 2,300. Numerous articles were found for TSSTs with inlet  $Re$ 's in the laminar or  $Re$ 's just in the transition flow regime. The earliest of these studies was by Lavan and Thompson, in which flow rates just entered in the turbulent regime. The results developed a correlation for extraction efficiency that used the aspect ratio,  $Gr$  number, and  $Re$  number (Eq. 20, **Table 2**) [90].

Cornelius et al. pilot-tested a passive thermal solar array at laminar flow rates and found the stratification in the tank significantly impacted the flow rate and performance of the passive system [65]. In a dissertation, Abdoly created a model for laminar flows in insulated and uninsulated tanks [66]. In two papers, Oppel et al. used the  $Re/Ri$  relationship to characterize vertical and horizontal inlets at  $Re$  below 3,300 [67],[9]. Later, Zurigat et al. improved on these studies with additional inlet configurations at these same flow rates [10], [68], [69]. Hariharan et al. developed a correlation (equation similar to that from Lavan and Thompson [55] for horizontal inlets) and noticed the  $Re$  number had a higher impact at lower temperatures [70]. This finding suggests the physical parameter viscosity and turbulence level described by the  $Re$  term is important to internal mixing within TSSTs.

Spall studied chilled water tanks with laminar inlet values and found that for  $Re$  between 30 and 3,000, the Archimedes number should be greater than 2 for stable stratification [74]. Hahne and Chen studied charging of solar thermal storage and found the  $Ri$  number and  $Pe$  number able to describe the laminar system—when  $Ri$  was greater than 0.25, the charging efficiency was >97% [75]. Nelson et al. created mixing parameters for sections of the tank at laminar flow rates and included the Biot and  $Pe$  numbers [58]. Van Berkel et al. studied laminar flows inside a rectangular tank with visualization techniques and confirmed the  $Ri_c$  of 0.25 when and a superficial  $Ri$  of 15 (using inlet velocity) as adequate for design of these geometries and laminar flow rates. The cycle thermal efficiency increased from 95% to near 99% at higher  $Ris$  [60]. Shah and Furbo tested and modeled three inlet types for laminar flow rates and found the  $Ri$  to relate to the exergy changes [71]. Panthaloorkaran et al. characterized TSSTs with the first and second laws of thermodynamics, and they suggested their model could be incorporated into CFD [72]. Kaloudis et al. modeled flow in a rectangular tank with large-eddy CFD for laminar flow rates [17]. Njoku et al. reviewed many laminar modeling methods and suggested the entropy generation number for modeling TSSTs [76]. Padovan et al. created a model for a tank with a coil at the bottom of the tank for seasonal storage modeling [77]. Tinaikar et al. studied the injection of a negative buoyant jet through a cone at the top of a TSST and how eddies affected the thermocline region while using the  $Ri$  to characterize the thermocline [49]. Kaloudis et al. studied cold laminar currents in a rectangular space that ran along the bottom of the wall and crashed into the far-side container wall [50]. Most recently, Capocelli et al. [44] studied a tank with stratified thermal oil at  $Res$  associated with the laminar flow or transitioning to turbulent flow in the pipe or tube before the inlet due to the high thermal diffusivity of the oil; the  $Pe$  number was also chosen.

These laminar studies are all valid for the geometry studied and the thermocline described within the specific study. Most cold-water flows into a tank are turbulent in a round-tube or pipe before entering the tank. These features significantly affect the possibility of an analytical solution, and most tank bottoms are round; the cold water takes a radial path before hitting an opposing wall.

Few articles were found in which the tube-inlet flow regimes in the transition to the turbulent range (e.g.,  $Re$  values greater than 2,300 for round tube geometry). Zurigat et al. expanded on Oppel's and his earlier studies to study the impact of  $Re > 2,300$  on vertical inlets that impinged the top of the tank to have a

perforated inlet and a side inlet. These were correlated to a function of  $Re/Ri$ , and the impinging inlet had the highest performance at these turbulent levels. Furthermore, to expand the research apparatus use and increase the density gradient, saline water was used for larger  $Ri$ 's [73]. An early CFD model was created by Mo and Miyatake using the k-epsilon turbulence model in an upwind scheme at turbulent inlet values [42]. Jordan and Furbo modeled a solar thermal stratified storage tank system with a half-circle baffle to redistribute the cold-water inlet jet at the bottom of a tank. Besides this novel inlet, two coiled heat exchangers in the tank delivered heat from the solar thermal array; the results were dependent on geometry and initial tank conditions [33]. Jordan and Furbo iteratively solved for a distance from the source in which mixing occurred called a mixing height, which is a volume of water in which the incoming water is perfectly mixed by using a jet width from a 2D CFD model as its characteristic length; the authors concluded this was analogous to using the  $Ri$  [33]. Their work further suggests the need for empirical factors based on inlet type and property-based factor for the initial conditions of the TSST. Gao used a 3D CFD model to determine the mixing height and applied an entrainment factor to the energy balance for the capture (mixed) volume near the inlet for different velocities [79]. Baeten et al., in a 2D CFD model, found the mixing to be linearly related to  $Re$  and height of mixing related to the aspect ratio,  $Re$  number, and  $Fr$  number [45]. The inverse square relates to the convection-based Froude number and  $Ri$  number, and the choice of using this or other convection numbers in tandem with the  $Re$  number is discussed in later sections. Njoku et al., in an overview, also examined models with turbulence levels in the inlet tube in which the eddy conductivity factor or eddy diffusion or mixing number was used to model the turbulence [76]. Most recently, Elatar et al.—in a 3D k-epsilon CFD model at high  $Re$  values associated with cold-inlet flows greater than 3 GPM—mapped the initial mixing velocity profiles, which created circulation at various levels within the whole in the tank [91]. Zurigrat et al. used the  $Re$  and  $Ri$  in a  $Re/Ri$  relationship to identify an eddy diffusivity factor that was an exponential function of height, with the larger values being close to the tank inlet in a 1D empirical model [73].

### 3.2 Convection and conduction numbers

The  $Pe$  number has been used to relate the advection to conductive diffusion in the water in a few articles. Kaloudis et al. used  $Pe$  in a laminar rectangular tank study and 3D simulation [17]. Nelson et al. used  $Pe$  to represent the conduction through the thermocline region as a ratio of the energy passing through the thermocline [58]. Tarawneh and Homan found an effective-diffusivity ratio for salt water that scaled on the  $Pe$  for a horizontal slot inlet at the bottom of a rectangular TSST [59]. Mo and Miyatake used  $Pe$  in their CFD model to represent the conduction effects in the water to that of the convection of the flowing water [42]. Homan's integral solution for TSST modeling included combining the thermal and eddy diffusivity into a thermal-mixing factor and then dividing it by  $Pe$ , in which appropriate laminar and turbulent conditions of the eddy diffusivity could be identified [61]. Brown et al. create a novel cylindrical porous inlet manifold and at small inlet velocities modeled and found  $Pe$  and  $Ri$  to be the most important factors in the control and formation of TSSTs for this inlet [62]. Njoku et al. used a 2D CFD model that spanned highly laminar to transition-turbulent  $Re$  values to quantify the effect of  $Pe$  and  $Ri$  on entropy generation [24]. The study analyzed a negatively buoyant hot-water inlet creating RT instabilities at the top of a tank and found the highest entropy generation was due to the stratified region for the laminar and near-laminar cases. The trend suggests a reversal of their findings at highly turbulent values and low  $Pe$  (e.g.,  $Pe = 5$  or less) [24]. Other authors also noted in studies in which the flow in the tube was laminar that at higher flow rates, the 1D and computational models started diverging from experimental results [58], [60].

Many papers used the  $Fr$  to characterize TSSTs [45]–[51]. Park et al. chose the  $Ri$  for analysis in oceanic studies and noted other authors using the overturn  $Fr$ , which is the square root of the inverse of the  $Ri$  [38]. The difference in  $Ri$  and this version of  $Fr$  is only scale, which can be advantageous in similitude studies. Tinaikar et al. introduced the use of  $Fr$  in literature and quantified the effects of a round nozzle injecting slugs of water that impacted the thermocline region in a CFD study. Although discussing  $Fr$ , Atwood, and  $Re$  numbers, they reported their findings in the form of  $Ri$  alone [49]. Kaloudis et al. varied the what they called the “inlet  $Fr$ ” from 0.05 to 2.00 ( $Ri = 14.1$  to 0.71) in a 2D CFD simulation of cold

water running along the bottom of a rectangular tank before the inlet wave crashed into the opposing wall [50]. Baeten et al. used the characteristic length of the tank diameter instead of the inlet diameter when using  $Fr$  in eight CFD studies that found the mixing rate was a function of  $Re$  number only. Baeten et al. developed a three-coefficient correlation (Eq. 25) for horizontal inlet into a round tank. In many models, the error in the initial state or final state is significant (e.g.,  $>20^{\circ}\text{C}$ ) at the hottest or coldest temperature—this model suffered from significantly underrepresenting the initial mixing. However, at times  $>150$  s, the reported normalized root mean square errors were between 1% and 7% ( $\sim 0.35^{\circ}\text{C}$  to  $2.45^{\circ}\text{C}$ ) [45]. For comparison, recent studies with empirical  $Re/Ri$  1D models reported root mean square errors no lower than 2.9% ( $1^{\circ}\text{C}$ ) [92] but compute in a fractions of seconds [41] compared with the days of calculations required for the 3D CFD models. In a chilled water TSST, Karim tested a novel large octagonal diffuser (that included small round holes along its perimeter) at laminar flow rates in a rectangular tank and concluded that diffusers should be designed based on a  $Fr$  value = 1 ( $Ri = 1$ ) and equal pressure drop [46], which creates evenly distributed flow to the small holes. The  $Ri$  value of unity is sometimes used as a transition to significant mixing that occurs at the strict definition of 0.25 ( $Fr = 16$ ); it is uncertain how the translation of this geometry and superficial use of velocity translates to the strict definition of the  $Ri$  number. In a seminal work in two parts by Jirka, turbulent buoyant jets into stratified media were modeled using  $Fr$  [93]. Similarly, Frick et al. closed one form of the plume equations using  $Fr$  for atmospheric studies [94]. These model could be converted to using  $Ri$ , but tanks are bounded, and these models are very limited in their applicability for TSSTs and especially for nonstandard inlet geometries and impinging jets on round surfaces commonly found in TSSTs.

Shin used the  $Fr$  and  $Re$  for laminar flows below  $Re = 800$  and  $Fr < 2$  ( $Ri > 14.4$ ) to study perforated diffusers in the top and bottom of the tank [47]. In a chilled water system, Bahnfleth et al. chose both  $Ri$  and the  $Fr$  to represent a large octagonal distributor with slot diffusers and showed that the superficial  $Ri$  number and Archimedes number were equivalent in this case [51]. In a similar application, Tang et al. studied large octagonal diffusers with nozzles at  $Fr = 0.45$  ( $Ri = 1.5$ ) instead of holes at laminar flow rates and found an improvement in storage efficiency from 80% to 90% with use of the nozzles on the distributor [48].

When flow measurements are a large source of error in the system, choosing the  $Fr$  will reduce the error in velocity. The  $Gr$  number is a popular choice for modeling the effects of heat loss through the tank walls and convection in the tank—notably,  $Gr$  is related to  $Re$  and  $Ri$  (equation 1).

$Gr$  is typically used when a surface is heated to determine heat transfer based on forced and free convection. The development of correlations for heated walls has been developed [52] and extended in recent CFD studies [56].  $Gr$  can be related to  $Ri$  number by

$$Gr = RiRe^2 \quad (1)$$

and was used [90] to characterize the extraction efficiency of TSSTs in the laminar and early transition  $Re$ 's (Eq. 15). In a TSST with a mantle heat exchanger wrapped around the tank, a high  $Gr$  in the mantle heat exchanger was found to preserve stratification in the tank [53]. In a chilled water study, Lake and Rezaie [25] used  $Gr$  as an intermediate calculation for  $Ri$  without considering the inlet geometry.  $Gr$  was used to identify the flow regime (turbulent or laminar) due to heat loss to the ambient for 10 geometrical shapes for a TSST [54]. Many articles use  $Gr$  in modeling the convection inside TSSTs. Notably,  $Gr$  is commonly used to identify heat loss or as an intermediate step to calculate  $Ri$  (Eq. 1). Other correlations based on  $Re$  and  $Ri$  are discussed in Section 3.1.

The Archimedes number ( $Ar$ ) defines the relationship of the gravitational forces to the viscous forces in fluid dynamics, and it can be equivalent to  $Ri$  for rectangular-slot diffusers using an inlet flow rate per unit length assumption [51].  $Ar$  was used by Spall in a 2D model and is listed as a critical value when the

value is greater than unity, and a strong contribution from buoyancy can be expected for laminar flow regime [74]. Jordan and Furbo used  $Ar$  as an intermediate step to calculate  $Ri$  [33]. Conversely, in a CFD k-epsilon model, Mo and Miyatake studied turbulent inlet flows at  $Re = 5,000$  for different  $Ar$  values and found no relationship between  $Ar$  to  $Re$  in a 2D k-epsilon model. Mo and Miyatake concluded that a 1D plug-flow model was valid at high  $Ar$  and invalid at low  $Ar$  [42]. For TSSTs, a low  $Ar$  corresponds to high turbulence.

The Biot number was used early in modeling stratification in tanks when thermal conduction through the walls results in significant temperature drops. Typically, the Biot number can be used to determine if lumped capacitance methods are appropriate for a system. The conduction in water is usually much slower than what it allows for the application of lumped capacitance solutions. Nelson et al. showed that the degree of thermal stratification can be expressed in terms of modified Biot number, which relates to the convection at the wall and to the axial conduction and longitudinal conduction down the wall; the study compared the length of the wall with thickness ratios for fiberglass, steel, and aluminum tanks [84]. Other CFD studies include the Biot number to model the conductivity in the water but the size of the term associated with the uber was not quantified.

The  $Ra$  number is commonly used for free convection and can also be an appropriate choice for convection modeling. When the  $Gr$  is used with  $Pr$ , the multiplication of these numbers is the definition of  $Ra$ , and the effect of fluid properties based on temperature can be studied. Kaloudis et al. found that in TSSTs,  $Ra$  varies from about 3.5 to 8 [17].  $Ra$  is the combination of all numbers required to describe the individual phenomenon in TSSTs and typically characterizes the onset of natural convection. This number appears to be the best choice for TSSTs but does not directly include critical numbers for the different types of mixing involved in TSSTs. Fan and Furbo used  $Ra$  to describe the heat loss from a tank due to ambient conditions [100]. In a dissertation, Newton used  $Ra$  in the classic fashion to quantify the heated natural convection to that of the thermal conduction [101].

### 3.2 Quiescent fluid numbers

The Atwood number is the heavier fluid subtracted from the lighter fluid divided by the sum of the densities and is used to characterize the strength (ability to reduce horizontal velocities) of the interface between two fluids. Tinaikar et al. used the Atwood number to characterize the strength of the thermocline and shot slugs of water through the thermocline creating vortexes, which were then related by  $Ri$  by adding in gravity and a characteristic length [49].

Levels of stratification quality are not often specified directly as a vertical height of a thermocline and can more generally be characterized by a stratification number ( $Str$ ) that relates thermal vertical gradient (at a location, time, or weighted average for the tank) to the maximum vertical gradient.

$$Str = \frac{\partial T / dy}{(\partial T / dy)_{T_H to T_C}} \quad (2)$$

The  $Str$  helps quantify the stratification strength (at the location, time, or tank average evaluation) to the maximum stratified region  $(\partial T / dy)_{T_H to T_C}$ , which is often applied for the tank height between the inlet and outlet ( $T_H$  or  $T_C$ ). Tinaikar et al. reported that the  $Str$  increases with increasing  $Ri$  [49]. Kumar et al. used this  $Str$  while including PCM spheres inside a hot water tank to determine the effect on stratification and found the over time, both the  $Str$  and  $Ri$  showed differences between the PCM and non-PCM system [88]. Fan and Furbo correlated the heat loss at the wall for each stratified node to the gradient  $Gr(I)$  in

$$Loss_i = 0.25Gr(I)^{-0.6} \quad (3)$$

which has the same numerator as the  $Str$  but is the distance between two nodes in the denominator [13]. In later studies, Fan and Furbo found that when the tank is poorly stratified, the temperature gradient is  $< 2$  K/m, and the downward fluid velocity is 0.003 to 0.015 m/s on the side wall and is related to gradient by

$$v = 0.0021Gr(I)^{-0.838} \quad (4)$$

for 100 to 500 L tanks and aspect ratios (tank height to diameter) ranging from 1 to 5 [64], [89]. Most domestic TSSTs have aspect ratios ranging from 1 to 4, and these correlations need to be used carefully because determining the gradient in the thermocline region is nontrivial in modeling TSSTs.

Stratification due to additional components in TSSTs has also been studied. The use of neutrally buoyant spheres full of PCMs [22] and tanks with a heating coil to heat the water [7], [45] are areas of interest for thermally stratified thermal storage. In a solar thermal system, Jadhav et al. reported the capital investment can reduce by 28% by stratifying the tank [31].

Many dimensionless numbers have been used to characterize stratified tanks.  $Ri$  has been studied extensively in stratified media such as salt water in the ocean or air in the atmosphere and in stability studies of thermoclines [32], [38].  $Ri$  is reviewed in more detail in the following section for use in TSST modeling.

### 3.3 The Richardson number

Many authors also use  $Ri$  (Table 1). The literature on using  $Ri$  is more expansive than literature found for  $Fr$  for quantifying inlet mixing phenomena in the thermocline region.  $Ri$  number also has many forms represented in tank water research, such as gradient local and semi-local (overall) discussed in a series of publications by Van Berkel et al. [60], [85]. The Archimedes, Atwood,  $Gr$ , and  $Fr$  numbers can be mathematically related to the  $Ri$  number.  $Ri$  describes the effect of buoyancy forces on a fluid flow that is at a different density than that of the quiescent fluid. The strict definition (gradient form) of  $Ri$  characterizes the buoyancy forces, or potential energy, to the density gradient and characterizes the flow shearing forces, or kinetic energy, by the velocity gradient of the fluid [78]. The characteristic velocity is that which is perpendicular to the gravity forces (Figure 3, A). Whitehead et al. discussed continuously stratified experiments in which the  $Ri$  can be defined as a critical number for stability analysis ( $Ri_c$ ),

$$Ri_c = \left( \frac{Nd}{u^*} \right)^2 \quad (5)$$

where  $N$  is the wave number,  $d$  is the distance of the stratification and  $u^*$  is the velocity scale of the turbulence [32].  $N$  is often unmeasured in TSST studies, and the horizontal velocity causes internal waves at the boundary layers between two fluids (KH1). The  $Ri$  number has been used in a large eddy simulation with the Kronecker delta to follow the path of an internal wave and quantify the impact on this mixing on thermocline height in a rectangular tank [82].

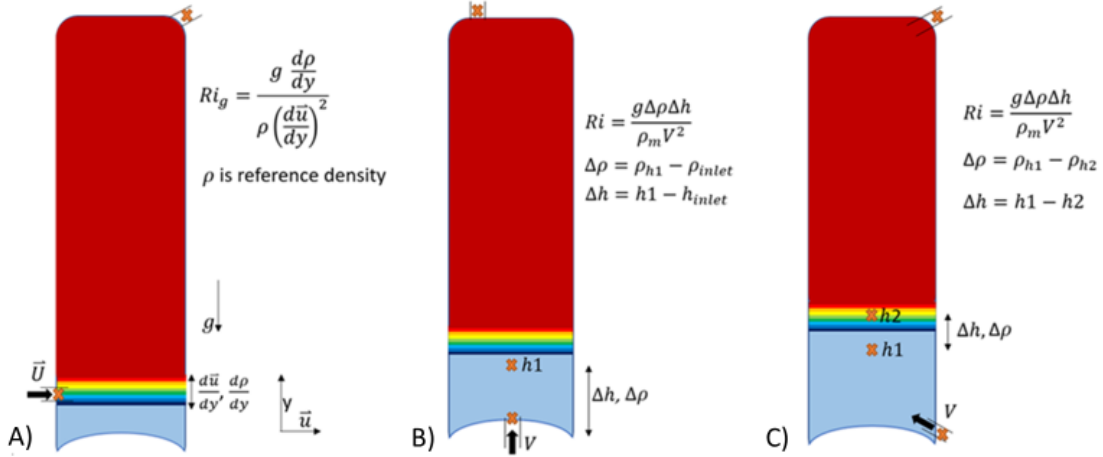


**Figure 3** Common uses of  $Ri$  in tank stratification modeling from (A) the strictest definition to (B) superficial use for inflow from below the thermocline and (C) arbitrary inlet flow direction with right being a quasi-local  $Ri$  evaluated in the thermocline.

The strict definition can use different length scales (**Table 3**) to identify the mixing along a horizontal plane due to shearing forces by eddies at the top and bottom of the thermocline. In many 1D models, the strict definition is relaxed, and the average inlet velocity, or superficial velocity, is often used in **Figure 2** (B) and (C).

Figure 3, (B) has been studied with flow visualization by Van Berkel et al. using the strict  $Ri$  definition and a slot diffuser [85], [86]. Velocities, locations of parameter evaluations, and thermocline location for  $Ri$  are shown in **Table 2** with the corresponding equations and reference(s).

The different uses of velocity in the literature and location of property evaluation makes it difficult to compare a study with a horizontal inlet (**Figure 3** (A)) with one with a vertical inlet (**Figure 3** (B), (C)) by a  $Ri_c$  alone, and the internal waves are often uncategorized. Most authors using  $Ri$  for TSSTs use the inlet temperature and the closest temperature sensing device as the location for property evaluation, whereas some use a local  $Ri$  between two sensors in a tank such as  $h1$  and  $h2$  in **Figure 3**(C). In **Table 2**, the various uses of  $Ri$  are compared, and the characterization relationship developed is shown. With flow visualization techniques, the strict definition can be directly measured [86]. In models, it can also be computed if the inlet jet is characterized well in terms of momentum and buoyancy flux [93].

The used of  $Ri$  in the literature characterization or modeling can be split into five categories: (1) the strict definition using horizontal velocity gradient, (2) thermal diffusivity for  $Re$  above approximately 3,300, (3) specific heat for  $Re$  below approximately 3,300, (4)  $Gr$ ,  $Fr$ , or  $Pe$  relationship  $Re$  below  $\sim 3,300$  and (5) velocity modification for  $Re$  below  $\sim 2,000$ . **Table 2** presents the associated literature with each category.

The strict or gradient use of  $Ri$  results in consistent findings for the critical value and unambiguous use of velocities. Flow visualization is often required to determine the horizontal velocity gradient, or the momentum equation is solved for classical outlet flows (e.g., plume in cross flow) [34] [80] [86].

The superficial use of  $Ri$  yields four distinct methods that have been used for TSSTs, and the  $Re$  cutoff that separates the use of these methods is about  $Re = 3,300$ . For  $Re$  above 3,300, modifying the thermal diffusivity in eddy diffusion equations has been successful in some studies [9], [10], [40], [67]–[69]. For  $Re$  below 3,300, modification to the specific heat for use in first-law energy balances has been successful in other studies [46], [81], [84]. Also, for  $Re$  below 3,300,  $Gr$ ,  $Fr$ , or  $Pe$  have been successfully used [45], [62], [90] For  $Re$  below about 2,000, modifications to velocity difference between the thermocline and the bulk of the fluid have been successful [60], [85], [86].

Table 2 Ri used in stratified thermal tanks and the quantitative or qualitative statements made about the Ri effect on thermal stratification or performance.

Reference(s)/ description	Characteristic, locations, lengths, and velocities	Richardson equation	Characterization relationship developed
Strict definition of Ri (horizontal velocities)			
[34] Horizontal jet into density- stratified reservoir	$U$ = horizontal jet velocity $dy$ = vertical differential length $D$ = width of jet $d\rho$ = evaluated over $D$ $\rho_0$ = reference density $\frac{d\rho}{dy}$ = gradient of density $\varepsilon_H$ = eddy conductivity	$Ri = \frac{g \left(\frac{d\rho}{dy}\right)}{\rho_0 \left(\frac{U}{D}\right)^2} \quad (5)$	$v \frac{\partial \bar{T}}{\partial y} = \frac{\partial}{\partial y} \left[ (\alpha + \varepsilon_H) \frac{\partial \bar{T}}{\partial y} \right] \quad (6)$
[86] Vertical slot diffuser	$u$ = velocity in the horizontal direction $y$ = vertical coordinate pointing down $dy$ = vertical differential length $d\rho$ = evaluated over $dy$ $\rho$ = reference density	$Ri_g = \frac{g \frac{d\rho}{dy}}{\rho \left(\frac{du}{dy}\right)^2} \quad (7)$	$Ri_g$ directly measured from experimental flow visualization
[80] Horizontal round jets	$G_c$ = modified local gravity $\dot{V}$ = the volumetric flow rate $\dot{M}$ = kinematic momentum flux $l$ = a characteristic length (see <b>Table 3</b> ) $u$ = horizontal velocity $b$ = jet width $F$ = stabilizing force $\beta = 2.2$ $z$ = vertical height $m$ = level maximum buoyancy $n$ = level neutral buoyancy	$Ri_l = \frac{G_c \dot{V}}{\sqrt{32\pi \dot{M}^5}} \quad (8)$	$F = \varepsilon u Ri b^3 \quad (9)$ $\varepsilon = \varepsilon_0 \exp\left(\frac{-(z - z_{n,m})^2}{l^2}\right) \quad (10)$ $\varepsilon_0 = 0.15$ , half of that from Mott and Woods [95]
Thermal diffusivity modification ( $Re > \sim 3300$ )			
[9], [67] Vertical and horizontal diffusers	$V$ = tank velocity bulk $\Delta\rho = \rho_{\text{initial}} - \rho_{\text{inlet}}$ $L$ = height from inlet to outlet $\rho_{avg}$ = average of $\rho_{\text{initial}}$ and $\rho_{\text{inlet}}$	$Ri = \frac{\Delta\rho g L}{\rho_{avg} V^2} \quad (11)$	$EDF = a \left(\frac{Re}{Ri}\right)^b \quad (12)$
[10], [68], [69] Vertical and horizontal diffusers	$U_{in}$ = normal inlet velocity $\Delta\rho = \rho_{\text{initial}} - \rho_{\text{inlet}}$ $h$ = height inlet to the bottom thermocouple $\rho_m$ = average of $\rho_{\text{initial}}$ and $\rho_{\text{inlet}}$	$Ri = \frac{\Delta\rho g h}{\rho_m U_{in}^2} \quad (13)$	$EDF = a \left(\frac{Re}{Ri}\right)^b \text{ when } Ri \leq 5 \quad (14)$

[40] Vertical round, slit and turning vane diffusers	$U_{in}$ = normal inlet velocity $\Delta\rho = \rho_{initial} - \rho_{inlet}$ $h$ = height inlet to the bottom thermocouple $\rho_m$ = average of $\rho_{initial}$ and $\rho_{inlet}$	$Ri = \frac{\Delta\rho gh}{\rho_m U_{in}^2} \quad (13)$	$EDF = a \left( \frac{Re}{Ri} \right)^b$ $b = f(\text{diffuser type})$ $a = f(\text{insertion depth}) \quad (15)$
Specific heat modification ( $Re < \sim 3300$ )			
[84] Chilled water vertical slot diffusers	$U_{in}$ = bulk vertical flow in the tank $\Delta T$ = initial temperature difference $\beta$ = average coefficient of thermal expansion $L$ = length of the storage tank	$Ri = \frac{g\beta\Delta TL}{\nu^2} \quad (16)$	$Z = 1.68 \times 10^4 \left( \frac{Re}{Ri} \right)^{0.67} \quad (17)$
[46], [81] Chilled water vertical round diffusers	$V$ = inlet velocity $\Delta T$ = initial temperature difference $\beta$ = average coefficient of thermal expansion $L$ = length of the storage tank	$Ri = \frac{g\beta\Delta TL}{U_{in}^2} \quad (18)$	When the thermocline is developed $Z = -3 \times 10^7 U_{in} + 254,526 \quad (19)$
$Gr, Fr,$ or $Pe$ relationship ( $Re < \sim 3,300$ )			
[90] Vertical diffusers	$Gr_D$ = Grashof number for the tank $Re_d$ = Reynolds number for the inlet $D$ = diameter of the tank $H$ = height of the tank $\eta$ = extraction efficiency	$Ri = \frac{Gr_D}{Re_d^2} \quad (1)$	$\eta = 1 - \exp \left[ -0.067 Re_d^{-0.55} Gr_D^{0.35} \left( \frac{H}{D} \right)^{0.58} \right] \quad (20)$
[70] Horizontal diffusers	$Gr_D$ = Grashof number for the tank $Re_d$ = Reynolds number for the inlet $D$ = diameter of the tank $L$ = height of the tank $\eta$ = extraction efficiency	$Ri = \frac{Gr_D}{Re_d^2} \quad (1)$	$\eta = 0.745 Re_d^{0.088} Gr_D^{-0.043} \left( \frac{L}{D} \right)^{0.229} \quad (21)$
[62] Porous vertical diffuser	$U_{in}$ = velocity inlet $R$ = radius of tank $T_{in}$ = initial temperature $T_i$ = initial tank $l$ = height of the tank $Pe$ = Peclet number	$Ri = \frac{g\beta R(T_{in} - T_i)}{U_{in}^2} \quad (22)$	$\frac{dT}{dz} = 5.3 + 2.235 Ri - \frac{38,422.42}{Pe} \quad (23)$
[45] Wrapped storage tank	$U_{in}$ = normal inlet velocity $\Delta T = T_{inlet} - T_{tank}$ $D$ = diameter of the tank $d$ = diameter of the inlet $\beta$ = coefficient of thermal expansion at the inlet	$\frac{1}{Fr^2} = Ri = \frac{g\beta \frac{D}{d} \Delta T}{U_{in}^2} \quad (24)$	$\frac{\delta Z_{mix,in}}{D} = A Re \frac{D^{0.5}}{d} Fr^n \exp \left[ -B Re \frac{D^{0.5}}{d} \right]$ $A = 7.090 \times 10^{-6}$ $B = 0.203 \times 10^{-6}$ $n = 1.343 \quad (25)$

Velocity modification ( $Re < \sim 2,000$ )			
[60], [85] Vertical slot diffuser	$U_{in}$ = normal velocity inlet $\Delta\rho = \rho_{inlet} - \rho_{outlet}$ $h$ = height between two measurement points $\rho_m$ = average of $\rho_{inlet}$ and $\rho_{outlet}$ $U_{th}$ is the bulk velocity of the thermocline	$Ri_H = \frac{\Delta\rho gh}{\rho_m U_{in}^2} \quad (13)$	$U_{th} = U_e + U_{in} \frac{A_{in}}{A_{tank}} \quad (26)$ $Ri_h = \frac{U_{th}}{U_e}, \text{ when } U_e \ll U_{th}$
[86] Vertical slot diffuser	$U_{in}$ = normal velocity inlet $\beta$ = evaluated at average thermocline temperature $h$ = relative height of thermocline $\Delta T = T_{h1} - T_{h2}$ $E$ = entrainment rate	$Ri_h = \frac{g\beta\Delta T h}{u_{in}^2} \quad (27)$ $Ri_h = \frac{U_{in}}{U_e}$	$E = \frac{U_e}{U_{in}} = C \frac{A_{in}}{A_{tank}} Ri_h^{-1} \quad (28)$ <p>C = 1 (no net buoyancy flux) or 0.5 (constant temperature boundary equal to lowest layer)</p>

The correlations are useful for the velocity ranges, geometry, and fluids examined. Notably, the transition to turbulent flow starts at  $\sim 2,300$  for fluids in round tubes. The cutoff of the correlations happens at approximately  $Re = 3,300$ , suggesting that in the early stages of the transition regime, the turbulence in the inlet devices is dissipated quickly. When the turbulence is significantly large, only seven studies successfully used these correlations for modifying thermal diffusivity [9], [10], [40], [67]–[69].

A local  $Ri$  was used in a model by Steinert et al. [80] to develop a quasi-1D model based on the momentum flux and volumetric flow rate for horizontal jets in a stratified medium. Steinert et al.'s work [80] relied on jet characterization presented by Jirka [93]. When the appropriate length scales are applied for inlet jets, the initial inlet flow pattern, with-out reflection off tank walls, can be described by  $Ri$ .

### 3.4 Stability and the Richardson number

Stability has been heavily researched in the atmospheric sciences and oceanography using the  $Ri_c$ . The conclusions offered are for turbulence  $Ri_c$  on the order of  $<1$  in both oceans and air, with most papers site the  $Ri_c$  as 0.25 [32],[96]. The  $Ri_c$  is the maximum value where turbulent flow and the associated entrainment mixing can survive. Where flow visualization was undertaken and  $Ri$  was measured directly, the same  $Ri_c$  was found [86]. Where flow visualization methods were not used, superficial velocity must be used, and the definition of  $Ri$  became specific to the geometry of the inlet, geometry of the tank, the location of the property evaluation, and most importantly, the velocity used in the relationship (**Table 2**).

Although the definitions and correlations in **Table 2** are different, they are useful for the specific system studied. A comparison of performance between systems by  $Ri_c$  alone leave discrepancies (**Table 3**) because the systems are not similar (e.g., inlet geometry, inlet flow direction [horizontal or vertical], or inlet-Reynolds number). When the strict definition is used for  $Ri_c$ , the classical critical number of 0.25 is reproduced [86]. When the measured  $Ri$  was calculated by van Berkel et al., the velocity of the inlet was used and length scale chosen was on the height of the tank and  $Ri_c$  was found to be near 20 instead of classic value of 0.25 [85]. Thus, the critical  $Ri$  value can be strict ( $Ri_{st}$ ) when visualized or superficial ( $Ri_{sf}$ ) when the inlet velocities and tank dimensions are used.

Table 3  $Ri_c$  from literature with designation of strict (st) or superficial (sf) definition used.

Reference(s)	$Ri_c$ inlet number	Inlet direction	Inlet type
[34]	$Ri_{st} < 0.25$ is unstable	Horizontal	Round jet
[10], [68], [69]	$Ri_{sf} < 3.6$ : mixing occurs $Ri_{sf} > 5$ : no mixing of the thermocline	Horizontal Vertical	Jet and diffuser
[60], [85]	$Ri_{sf} > 20$ : 5% mixing maximum	Vertical	Slot diffuser
[84]	$Re/Ri_{sf}$ should be minimized	Vertical	Round jet
[86]	$Ri_{st} < 0.25$ : significant turbulence $Ri_{sf} = 15$ : adequate design	Vertical	Slot diffuser
[51]	$Ri_{sf} > 100$ : negligible effect on the thermocline	Vertical	Slot diffuser
[62]	$Ri_{sf} = 0.651$ : stratification seen	Vertical	Porous diffuser
[45]	None found when spanning typical critical $Ri_{sf} = 0.25$	Horizontal	Round jet
[25]	$Ri_{sf}$ was $> 200,000$ and there was development of second thermocline from a chilled water diffuser	Vertical	Cone diffuser
[40]	$Ri_{sf} > 2.5$ is stable	Vertical	Round jet Slit-perforated horizontal jet Turning-vane distributor

$Ri_{sf}$  is specific to the system and the critical numbers from below 0.25 to 100 were found in the literature (**Table 3**). These differences are because of the definition used and the inlet directions, types and tank conditions. The three order of magnitude range in critical values suggest poor description of KH and RT instabilities when the superficial velocity is used to model the TSSTs.

Characterizing the phenomena using the strict definition of velocity perpendicular to the thermocline is reproducible and preferred for many inlet geometries. Correlations between the strict definition and superficial definition require flow visualization of TSSTs in many inlet geometries and aspect ratios. The authors do not know of any academic studies or industry attempts to resolve the strict and superficial definition of  $Ri$ .

#### 4. Discussion

Most authors use the height of the tank or height between two thermocouples in the  $Ri$  number calculation and are therefore using lengths on the order of the inertial scale for TSSTs. Using a local  $Ri$  with a fixed height on the inertial scale reduces the information provided by the  $Ri$ . Studies using PIV directly measure  $Ri$ 's number [85], [97] and do not refer to a scale and use the height of the thermocline as their characteristic length scale.

The  $Ri$  scale appropriate for analysis is different based on the phenomena occurring in TSSTs, and the height or diameter of the tank has been used by almost all researchers. A scale created by Mott and Woods that was later used by Steinart et al. is unnamed (UN) [80], [95]. With reflection and plumes, the appropriate length scale will change throughout the evolution of the flow from the inlet to the stratified region. A full list of scales that could be used with  $Ri$  is shown in **Table 4**.

Table 4 The length scales present stratified media.

Scale name	Characteristic length	Phenomenon	Reference(s)
Corrsin	$L = \sqrt{\varepsilon_d/S^3}$ (28)	Eddies are deformed by shear, plume regions	[98]
Ozmidov	$L = \sqrt{\varepsilon_d/N^3}$ (29)	Stability stratified region, eddies deformed by stratification	[98], [99]
UN	$L = \frac{\beta u}{\sqrt{(g/\rho_{ref})(\partial\rho/\partial y)}}$ (30)	Buoyancy limit in the stratified region	[80], [95]
Ellison	$L = \frac{-\rho'}{\partial\bar{\rho}/\partial y}$ (31)	Overturning scale, where $\rho'$ is reduced gravity	[99]
Monin-Obukhov	$L = -\frac{u_*^3}{\frac{\kappa G}{T} \frac{Q}{\rho C_p}}$ (32)	$u_*$ is the frictional velocity, $\kappa$ is the Von Kármán constant, $Q$ is the turbulent heat flux	[100]
Inertial scale	$L^* = D \text{ or } H$ (33)	Momentum jet maximum travel distance	All authors in <b>Table 2</b> unless specified otherwise

\*length assumed because no author using  $D$  or  $H$  referenced the inertial scale, and a jet hitting a tank wall perpendicular to the flow direction will cause large scale overturning due to shearing forces at the wall.

In **Table 4**,  $\varepsilon_d$  is the dissipation rate of turbulence,  $S$  is the shear rate,  $N$  is the KH frequency,  $\beta$  is a constant of proportionality, and  $u$  is the mean plume velocity. The inertial scale is assumed in **Table 2** as this scale would dominate in large-scale vertical overturning because of jets reflecting off walls. For small jets created locally by a multi-orifice diffuser, these length scales are too long.

Numerous articles were found that use  $Ri$  for analysis of the convection associated in TSSTs with various inlet geometries and flow rates. The stratified tank studies reviewed experience all jet and plume phenomena, and the most common length scale of tank diameter or height used in literature was on the order of the tank diameter or height of the tank. To describe the internal mixing in the tank, other scales listed may prove useful. During charging of the tank from an external heat source (e.g., building a thermocline), the Corrsin and then Ozmidov length scale characterize the initial mixing, entrainment, and layering phenomena. The Monin-Obuhov scale could be used when plumes of water with very different temperatures enter the stratified region.

There are many approaches to model TSSTs, many of which rely on nondimensional correlations based on experiments. Furthermore, the critical values of the correlation through the experiments are useful for modeling. The integration technique for the momentum balance [80], [93] was briefly reviewed, and with complex diffusers deflecting of tank walls, the flow paths are hard to verify without visualization. We hypothesize by the findings that at  $Re = 200$  to  $3,300$ , the turbulent eddies at the inlet of the vertical tube

inlet are easily dissipated at the stratified region. Furthermore, when transitioning to turbulence in the inlet tube, the sources of the eddies are stronger, or more established, and have a greater impact on the thermocline region, causing oscillations in the layer that create additional diffusion called eddy diffusion.

Modeling the stratification in tanks has been a complex technique due to the following reasons,

1. there are few selective dominant factors which are shared as common aspect for various platforms such as aspect ratio, inlet direction and flow rate,
2. the transition of turbulence in the inlet device to a quiescent fluid has analytical solutions for special unbounded cases only [40],
3. the disturbance to the stratified region can occur on at least two length scales (**Table 3**),
4. as the time scale increases, conduction plays a larger role (e.g., as conduction may be ignored in shorter time scales such as <8 h),
5. high gradient regions are computationally optimized by different methods than low gradient regions,
6. hot-water tanks have very different inlet devices, that can affect the flow patterns within the tank.

For these reasons, there have been many different models proposed to model TSSTs that are valid for the specific conditions, however, they cannot be generalized for all the other applications. The authors view the  $Re/Ri$  relationship by Oppel et al. as the best 1D approach to model TSSTs for a wide range of temperatures and inlet devices when there is turbulence in the inlet piping or vertical tube inlet [10].

## 5. Conclusions

The studies of stratified tanks has been a subject of interest for a while. As tank technology has improved, the phenomena of heat transfer through the walls have decreased, whereas the various vertical-tube inlet devices have expanded the relevance of Reynolds ( $Re$ ) and Richardson ( $Ri$ ) or the  $Ri$  related Froude ( $Fr$ ) and Grashof to characterize convection in 1D models. As the outer layer of hot water tanks becomes more complicated (e.g., wrapped by heat exchanging and two-phase flow tube in the case of wrapped heat pump water heaters), the complexity inside the tank increases. The use of the strict  $Ri$ , in combination with  $Re$ , is suggested for modeling thermally stratified storage tanks (TSSTs).

The Kelvin-Helmholtz (KH) and Raleigh-Taylor (RT) instabilities are the major drivers of short-term mixing in TSSTs. The internal waves and layering of similar density fluid in the horizontal plane create KH instabilities. RT instabilities from negatively or positively buoyant plumes, traveling with a vertical component, create entrainment mixing along the edges of the plume. Momentum jets deflecting off walls in the bottom of the tank also create significant entrainment mixing. Rayleigh number has the most property-based information of the nondimensional numbers reviewed but suffers from the same geometric constraints as  $Ri$  and  $Fr$  when using superficial velocity and furthermore is not related to KH and RT instabilities in the literature.

$Ri$  was found to adequately define the stratification hot-water residential or commercial tanks. The ratio of  $Re$  to  $Ri$  included the best empirical values for modeling TSTTs for a range of inlet devices and turbulent inlet values. Using superficial velocity in the calculation of  $Ri$  results in  $Ri_c$  values for TSSTs unrepresented by the classical value of 0.25, and the literature reports superficial  $Ri_c$  values ranging from below 0.25 to 100 for TSSTs. These ranges were because the inlet configurations were specific to the geometry and different jet types causing different instabilities and entrainment. Finally, a brief list of the major conclusions of the review is as follows:

1. The convection-based numbers reviewed in this paper relate to  $Ri$ , and we suggest conformal and strict use of  $Ri$  in modeling TSSTs with the characteristic length of tank diameter and use of the velocity only in the direction perpendicular to gravity because this has the largest impact on unification of the  $Ri_c$  values. The location of evaluation of the density is less critical but should be at the top and bottom of the thermocline for unifying  $Ri_c$  values.

2. The  $Re/Ri$  relationship was found to be most robust over a range of  $Re$  values found before the inlet. Evaluation of  $Re$  at the inlet in complex geometrics is difficult if not impossible, and empirical correlations are required for modeling the impact of inlet geometry.
3. The decay of the turbulent eddies is nonlinear when there is a source of turbulence prior to the inlet geometry (e.g., classically defined as  $Re > 2,300$  for round geometry), and studies showed that at  $Re > 3,300$ , models required fitting parameters. The length scale most often used was the diameter or height of the tank and was selected by which one was in the direct path from the inlet flow.
4. When  $Re < 3,300$ , a few geometries that minimized mixing in the thermocline region were only related to inlet velocity. In these cases, nondimensional numbers quantifying the quiescent fluid were very informative to the models. The correlations developed were nonlinear and geometry-specific.

This review brings together more than 50 years of research on TSSTs in solar-thermal, chilled-water, and hot-water domestic use cases. The models proposed were all valid for the conditions under which they were studied. For a comprehensive model TSST a convection number needs to be paired with geometric information. Furthermore, analytical solutions of the Navier-Stokes equations for TSSTs do not exist due to the complex geometry. CFD models were also valid for the flow rate and geometry with which they were studied, but they were costly in computation time. 1D models with empirical correlations are the most effective solution method for seasonal studies until analytical solutions are found for this complex phenomenon inside TSSTs used for solar-thermal, chilled-water, and domestic hot-water use cases.

## **Acknowledgments**

This project was supported in part by an appointment to the Oak Ridge National Laboratory Higher Education Research Experiences program, administered by Oak Ridge Associated Universities through the US Department of Energy Oak Ridge Institute for Science and Education.

This work was sponsored by the US Department of Energy's Building Technologies Office under Contract No. DE-AC05-00OR22725 with UT-Battelle, LLC. The authors would like to acknowledge Mr. Antonio Bouza, Technology Manager of HVAC&R, Water Heating, and Appliance, US Department of Energy Building Technologies Office.

The authors would also like to acknowledge Ce Shi [101] for the discussion of Richardson number and its relation to thermal storage tanks, and Fernando Karg Bulnes, a Building Technologies Research and Integration Center summer intern, for help with references.

## References

- [1] W. B. K. Thomson, “Hydrokinetic Solutions and Observations,” *Balt. Lect. Mol. Dyn. Wave Theory Light*, no. August, pp. 584–601, 2012.
- [2] Helmholtz, “XLIII. On discontinuous movements of fluids,” *London, Edinburgh, Dublin Philos. Mag. J. Sci.*, vol. 36, no. 244, pp. 337–346, Nov. 1868.
- [3] Lord Rayleigh, “LIX. On convection currents in a horizontal layer of fluid, when the higher temperature is on the under side,” *London, Edinburgh, Dublin Philos. Mag. J. Sci.*, vol. 32, no. 192, pp. 529–546, 1916.
- [4] G. S. Taylor, “The instability of liquid surfaces when accelerated in a direction perpendicular to their planes. II,” *Proc. R. Soc. London. Ser. A. Math. Phys. Sci.*, vol. 202, no. 1068, pp. 81–96, 1950.
- [5] D. A. Arias, A. C. McMahan, and S. A. Klein, “Sensitivity of long-term performance simulations of solar energy systems to the degree of stratification in the thermal storage unit,” *Int. J. Energy Res.*, vol. 32, no. 3, pp. 242–254, 2008.
- [6] Y. P. Chandra and T. Matuska, “Stratification analysis of domestic hot water storage tanks: A comprehensive review,” *Energy and Buildings*, vol. 187. Elsevier Ltd, pp. 110–131, 15-Mar-2019.
- [7] B. Shen, K. Nawaz, V. Baxter, and A. Elatar, “Development and validation of quasi-steady-state heat pump water heater model having stratified water tank and wrapped-tank condenser,” *Int. J. Refrig.*, vol. 87, pp. 78–90, 2018.
- [8] J. Lago, F. De Ridder, W. Mazairac, and B. De Schutter, “A 1-dimensional continuous and smooth model for thermally stratified storage tanks including mixing and buoyancy,” *Appl. Energy*, vol. 248, no. May, pp. 640–655, 2019.
- [9] F. J. Oppel, A. J. Ghajar, and P. M. Moretti, “Computer simulation of stratified heat storage,” *Appl. Energy*, vol. 23, no. 3, pp. 205–224, 1986.
- [10] Y. H. Zurigat, K. J. Maloney, and A. J. Ghajar, “A comparison study of one-dimensional models for stratified thermal storage tanks,” *J. Sol. Energy Eng. Trans. ASME*, vol. 111, no. 3, pp. 204–210, 1989.
- [11] O. Abdelhak, H. Mhiri, and P. Bournot, “CFD analysis of thermal stratification in domestic hot water storage tank during dynamic mode,” *Build. Simul.*, vol. 8, no. 4, pp. 421–429, Aug. 2015.
- [12] W. Yaïci, M. Ghorab, E. Entchev, and S. Hayden, “Three-dimensional unsteady CFD simulations of a thermal storage tank performance for optimum design,” *Appl. Therm. Eng.*, vol. 60, no. 1–2, pp. 152–163, 2013.
- [13] J. Fan and S. Furbo, “Thermal stratification in a hot water tank established by heat loss from the tank,” in *ISES Solar World Congress*, 2009, pp. 341–350.
- [14] A. Elatar, K. Nawaz, B. Shen, and V. Baxter, “Hydrodynamic behavior of wrapped coil water heater tank,” *Therm. Sci. Eng. Prog.*, vol. 20, no. May, p. 100741, 2020.
- [15] A. Li, F. Cao, W. Zhang, B. Shi, and H. Li, “Effects of different thermal storage tank structures on temperature stratification and thermal efficiency during charging,” *Sol. Energy*, vol. 173, pp. 882–892, Oct. 2018.
- [16] C. Shi and P. Hrnjak, “Performance evaluation and validation of a novel heat pump water heater with rotary compressor and D-shaped condenser coils,” *Refrig. Sci. Technol.*, vol. 2019-Augus, no. 2014, pp. 4389–4398, 2019.
- [17] E. Kaloudis, D. G. E. Grigoriadis, E. Papanicolaou, and T. Panidis, “Large eddy simulations of turbulent mixed convection in the charging of a rectangular thermal storage tank,” *Int. J. Heat Fluid Flow*, vol. 44, pp. 776–791, Dec. 2013.
- [18] Y. Bai, M. Yang, Z. Wang, X. Li, and L. Chen, “Thermal stratification in a cylindrical tank due to heat losses while in standby mode,” *Sol. Energy*, pp. 222–234, Jun. 2019.
- [19] Z. Wang, H. Zhang, B. Dou, H. Huang, W. Wu, and Z. Wang, “Experimental and numerical research of thermal stratification with a novel inlet in a dynamic hot water storage tank,” *Renew. Energy*, vol. 111, pp. 353–371, 2017.

- [20] F. Ju, X. Fan, Y. Chen, H. Zhang, T. Wang, and X. Tang, "Performance assessment of heat pump water heaters with R1233zd(E)/HCs binary mixtures," *Appl. Therm. Eng.*, vol. 123, pp. 1345–1355, 2017.
- [21] J. Wu, Y. Feng, C. Liu, and H. Li, "Heat transfer characteristics of an expanded graphite/paraffin PCM-heat exchanger used in an instantaneous heat pump water heater," *Appl. Therm. Eng.*, vol. 142, pp. 644–655, 2018.
- [22] Z. Wang, H. Zhang, H. Huang, B. Dou, X. Huang, and M. A. Goula, "The experimental investigation of the thermal stratification in a solar hot water tank," *Renew. Energy*, pp. 862–874, Apr. 2019.
- [23] H. Huang *et al.*, "An experimental investigation on thermal stratification characteristics with PCMs in solar water tank," *Sol. Energy*, vol. 177, no. October 2018, pp. 8–21, 2019.
- [24] H. O. Njoku, O. V. Ekechukwu, and S. O. Onyegebu, "Normalized charging exergy performance of stratified sensible thermal stores," *Sol. Energy*, vol. 136, pp. 487–498, Oct. 2016.
- [25] A. Lake and B. Rezaie, "Energy and exergy efficiencies assessment for a stratified cold thermal energy storage," *Appl. Energy*, vol. 220, no. March, pp. 605–615, Jun. 2018.
- [26] E. Saloux and J. A. Candanedo, "Modelling stratified thermal energy storage tanks using an advanced flowrate distribution of the received flow," *Appl. Energy*, vol. 241, no. March, pp. 34–45, 2019.
- [27] Y. Bai *et al.*, "Numerical and experimental study of an underground water pit for seasonal heat storage," *Renew. Energy*, vol. 150, pp. 487–508, May 2020.
- [28] Z. Zhang, P. Song, and Y. Fan, "Experimental investigation on the geometric structure with perforated baffle for thermal stratification of the water tank," *Sol. Energy*, vol. 203, pp. 197–209, 2020.
- [29] T. Chandra, Yogender Pal; Matuska, "Numerical prediction of the stratification performance in domestic hot water storage tanks." pp. 1165–1179, 2020.
- [30] B. Baeten, T. Confrey, S. Pecceu, F. Rogiers, and L. Helsen, "A validated model for mixing and buoyancy in stratified hot water storage tanks for use in building energy simulations," *Appl. Energy*, vol. 172, pp. 217–229, 2016.
- [31] I. B. Jadhav, M. Bose, and S. Bandyopadhyay, "Optimization of solar thermal systems with a thermocline storage tank," *Clean Technol. Environmental Policy*, vol. 22, no. 5, pp. 1069–1084, 2020.
- [32] J. A. Whitehead, "Laboratory Studies of Turbulent Mixing," in *Encyclopedia of Ocean Sciences*, Elsevier Ltd, 2010, pp. 371–376.
- [33] U. Jordan and S. Furbo, "Thermal stratification in small solar domestic storage tanks caused by draw-offs," in *Solar Energy*, 2005, vol. 78, no. 2, pp. 291–300.
- [34] A. Bejan, "Buckling flows: a new frontier in fluid mechanics," *Annu. Rev. Heat Transf.*, vol. 1, no. 1, pp. 262–304, Mar. 1987.
- [35] R. L. Cole and F. O. Bellinger, "Thermally stratified tanks," *ASHRAE Trans.*, vol. 88, pp. 1005–1007, 1982.
- [36] J. S. Turner, *Buoyancy Effects in Fluids*. Cambridge: Cambridge University Press, 1973.
- [37] R. Camassa *et al.*, "Optimal mixing of buoyant jets and plumes in stratified fluids: theory and experiments," *J. Fluid Mech.*, vol. 790, pp. 71–103, Mar. 2016.
- [38] Y. G. Park, J. A. Whitehead, and A. Gnanadeskian, "Turbulent Mixing in Stratified Fluids: Layer Formation and Energetics," *J. Fluid Mech.*, vol. 279, pp. 279–311, 1994.
- [39] J. D. Rendall, K. R. Gluesenkamp, W. Worek, A. Abu-Heiba, K. Nawaz, and T. Gehl, "Empirical characterization of vertical-tube inlets in hot-water storage tanks," *Int. Commun. Heat Mass Transf.*, vol. 119, p. 104838, Dec. 2020.
- [40] J. Rendall, "Thermal stratification in hot water tanks: a review, an empirical fit, a novel model and a prototype diffuser," Texas A&M University - Kingsville, 2019.
- [41] F. K. Bulnes, K. R. Gluesenkamp, and J. Rendall, "Comparison of plug flow and multi-node stratified tank modeling approaches regarding computational efficiency and accuracy," in *ASME*

- 2020 *International Mechanical Engineering Congress and Exposition*, 2020, pp. 1–9.
- [42] Y. Mo and O. Miyatake, “Numerical analysis of the transient turbulent flow field in a thermally stratified thermal storage water tank,” *Numer. Heat Transf. Part A Appl.*, vol. 30, no. 7, pp. 649–667, Nov. 1996.
- [43] J. E. B. Nelson, A. R. Balakrishnan, and S. Srinivasa Murthy, “Experiments on stratified chilled-water tanks,” *Int. J. Refrig.*, vol. 22, no. 3, pp. 216–234, 1999.
- [44] M. Capocelli, G. Caputo, M. De Falco, I. Balog, and V. Piemonte, “Numerical Modeling of a Novel Thermocline Thermal Storage for Concentrated Solar Power,” *J. Sol. Energy Eng.*, vol. 141, no. 5, p. 051001, Mar. 2019.
- [45] B. Baeten, T. Confrey, S. Pecceu, F. Rogiers, and L. Helsen, “A validated model for mixing and buoyancy in stratified hot water storage tanks for use in building energy simulations,” *Appl. Energy*, vol. 172, pp. 217–229, Jun. 2016.
- [46] M. A. Karim, “Experimental investigation of a stratified chilled-water thermal storage system,” *Appl. Therm. Eng.*, vol. 31, no. 11–12, pp. 1853–1860, Aug. 2011.
- [47] M. S. Shin, H. S. Kim, D. S. Jang, S. N. Lee, Y. S. Lee, and H. G. Yoon, “Numerical and experimental study on the design of a stratified thermal storage system,” *Appl. Therm. Eng.*, vol. 24, no. 1, pp. 17–27, Jan. 2004.
- [48] J. L. Tang, Z. R. OuYang, and Y. Y. Shi, “Experimental analysis and FLUENT simulation of a stratified chilled water storage system,” *Eur. Phys. J. Plus*, vol. 134, no. 3, Mar. 2019.
- [49] A. Tinaikar, S. Advait, U. K. Chetia, K. V. Manu, and S. Basu, “Spatio-temporal disruption of thermocline by successive laminar vortex pairs in a single tank thermal energy storage,” *Appl. Therm. Eng.*, vol. 109, pp. 924–935, Oct. 2016.
- [50] E. Kaloudis, D. G. E. Grigoriadis, and E. Papanicolaou, “Numerical simulations of constant-influx gravity currents in confined spaces: Application to thermal storage tanks,” *Int. J. Therm. Sci.*, vol. 108, pp. 1–16, 2016.
- [51] W. P. Bahnfleth, J. Song, and J. M. Cimbala, “Measured and modeled charging of a stratified chilled water thermal storage tank with slotted pipe diffusers,” *HVAC R Res.*, vol. 9, no. 4, pp. 467–491, 2003.
- [52] W. J. Minkowycz and E. M. Sparrow, “Heat Transfer Variable Diffusion in the Presence Resistance , and of Noncondensables , Interfacial,” *Int. J. Heat Mass Transf.*, vol. 9, pp. 1125–1144, 1966.
- [53] M. Arslan and A. A. Igci, “Thermal performance of a vertical solar hot water storage tank with a mantle heat exchanger depending on the discharging operation parameters,” *Sol. Energy*, vol. 116, pp. 184–204, Jun. 2015.
- [54] Z. Yang, H. Chen, L. Wang, Y. Sheng, and Y. Wang, “Comparative study of the influences of different water tank shapes on thermal energy storage capacity and thermal stratification,” *Renew. Energy*, vol. 85, pp. 31–44, 2016.
- [55] Z. Lavan and J. Thompson, “Experimental study of thermally stratified hot water storage tanks,” *Sol. Energy*, vol. 19, no. 5, pp. 519–524, 1977.
- [56] O. Garbrecht, “Large Eddy Simulation of Three-dimensional Mixed Convection on a Vertical Plate,” 2017.
- [57] H. O. Njoku, O. V. Ekechukwu, and S. O. Onyegegbu, “Comparison of energy, exergy and entropy generation-based criteria for evaluating stratified thermal store performances,” *Energy Build.*, vol. 124, pp. 141–152, Jul. 2016.
- [58] J. E. B. Nelson, A. R. Balakrishnan, and S. Srinivasa Murthy, “Transient analysis of energy storage in a thermally stratified water tank,” *Int. J. Energy Res.*, vol. 22, no. 10, pp. 867–883, Aug. 1998.
- [59] C. M. Tarawneh and K. O. Homan, “Measurements of density profile evolution during the stably-stratified filling of an open enclosure,” *Int. J. Heat Fluid Flow*, vol. 29, no. 4, pp. 1113–1124, 2008.
- [60] J. van Berkel, C. C. M. Rindt, and A. A. van Steenhoven, “Modelling of two-layer stratified

- stores,” *Sol. Energy*, vol. 67, no. 1–3, pp. 65–78, Jul. 1999.
- [61] K. O. Homan, “Integral Solutions for Transient Temperature Profiles in Stably-Stratified Open Enclosures,” *J. Heat Transfer*, vol. 125, no. 2, p. 273, Mar. 2003.
- [62] N. M. Brown and F. C. Lai, “Enhanced thermal stratification in a liquid storage tank with a porous manifold,” *Sol. Energy*, vol. 85, no. 7, pp. 1409–1417, 2011.
- [63] J. Newton, T. Mom, and S. Klein, “Modeling of Solar Storage Tanks,” Wisconsin-Madison, 1995.
- [64] J. Fan and S. Furbo, “Buoyancy driven flow in a hot water tank due to standby heat loss,” *Sol. Energy*, vol. 86, no. 11, pp. 3438–3449, Nov. 2012.
- [65] K. A. Cornelius, “The USAFA Solar Energy Research Project Summary Report,” El Paso County, 1980.
- [66] M. A. Abdoly, “Thermal stratification in storage tanks,” University of Texas at Dallas, 1981.
- [67] F. J. Oppel, A. J. Ghajar, and P. M. Moretti, “Numerical and experimental study of stratified thermal storage,” in *ASHRAE Transactions*, 1986, vol. 92, no. pt 2A, pp. 293–309.
- [68] Y. H. Zurigat, P. R. Liche, and A. J. Ghajar, “Turbulent mixing correlations for a thermocline thermal storage tank,” in *AIChE Symposium Series*, 1988, vol. 84, no. 263, pp. 160–168.
- [69] Y. H. Zurigat, A. J. Ghajar, and P. M. Moretti, “Stratified thermal storage tank inlet mixing characterization,” *ICHe Symp. Ser.*, vol. 93, pp. 160–169, 1989.
- [70] K. Hariharan, K. Badrinarayana, S. Srinivasa Murthy, and M. V. Krishna Murthy, “Temperature stratification in hot-water storage tanks,” *Energy*, vol. 16, no. 7, pp. 977–982, Jul. 1991.
- [71] L. J. Shah and S. Furbo, “Entrance effects in solar storage tanks,” *Sol. Energy*, vol. 75, no. 4, pp. 337–348, 2003.
- [72] V. Panthaloorkaran, W. Heidemann, and H. Müller-Steinhagen, “A new method of characterization for stratified thermal energy stores,” *Sol. Energy*, vol. 81, no. 8, pp. 1043–1054, Aug. 2007.
- [73] Y. H. Zurigat, P. R. Liche, and A. J. Ghajar, “Influence of inlet geometry on mixing in thermocline thermal energy storage,” 1991.
- [74] R. E. Spall, “A numerical study of transient mixed convection in cylindrical thermal storage tanks,” *Int. J. Heat Mass Transf.*, vol. 41, no. 13, pp. 2003–2011, Jul. 1998.
- [75] E. Hahne and Y. Chen, “Numerical study of flow and heat transfer characteristics in hot water stores,” *Sol. Energy*, vol. 64, no. 1–3, pp. 9–18, 1998.
- [76] H. O. Njoku, O. V. Ekechukwu, and S. O. Onyegebu, “Analysis of stratified thermal storage systems: An overview,” *Heat Mass Transf.*, vol. 50, no. 7, pp. 1017–1030, Jul. 2014.
- [77] R. Padovan, M. Manzan, E. Z. De Zorzi, G. Gulli, and A. Frazzica, “Model Development and Validation for a Tank in Tank Water Thermal Storage for Domestic Application,” *Energy Procedia*, vol. 81, pp. 74–81, Dec. 2015.
- [78] A. Bejan, *Convection Heat Transfer*. Hoboken, NJ, USA: John Wiley & Sons, Inc., 2013.
- [79] W. Gao, T. Liu, W. Lin, and C. Luo, “Numerical Study on Mixing Characteristics of hot Water inside the Storage Tank of a Solar System with Different Inlet Velocities of the Supply Cold Water,” *Procedia Environ. Sci.*, vol. 11, pp. 1153–1163, 2011.
- [80] P. Steinert, S. Göppert, and B. Platzer, “Transient calculation of charge and discharge cycles in thermally stratified energy storages,” *Sol. Energy*, vol. 97, pp. 505–516, Nov. 2013.
- [81] A. Karim, A. Burnett, and S. Fawzia, “Investigation of stratified thermal storage tank performance for heating and cooling applications,” *Energies*, vol. 11, no. 5, 2018.
- [82] E. Kaloudis, D. G. E. Grigoriadis, E. Papanicolaou, and T. Panidis, “Large eddy simulation of thermocline flow phenomena and mixing during discharging of an initially homogeneous or stratified storage tank,” *Eur. J. Mech. B/Fluids*, vol. 48, pp. 94–114, 2014.
- [83] R. V. K. Chakravarthy, L. Lesshafft, and P. Huerre, “Global stability of buoyant jets and plumes,” *J. Fluid Mech.*, vol. 835, pp. 654–673, Jan. 2018.
- [84] J. E. B. Nelson, A. R. Balakrishnan, and S. Srinivasa Murthy, “Parametric studies on thermally stratified chilled water storage systems,” *Appl. Therm. Eng.*, vol. 19, no. 1, pp. 89–115, Jan. 1999.
- [85] J. Van Berkel, “Mixing in thermally stratified energy stores,” in *Solar Energy*, 1996, vol. 58, no. 4–6, pp. 203–211.

- [86] J. van Berkel, C. C. M. Rindt, and A. A. van Steenhoven, "Thermocline dynamics in a thermally stratified store," *Int. J. Heat Mass Transf.*, vol. 45, no. 2, pp. 343–356, Jan. 2001.
- [87] A. Matulka, P. López, J. M. Redondo, and A. Tarquis, "On the entrainment coefficient in a forced plume: Quantitative effects of source parameter," *Nonlinear Process. Geophys.*, vol. 21, no. 1, pp. 269–278, Feb. 2014.
- [88] G. S. Kumar, D. Nagarajan, L. A. Chidambaram, V. Kumaresan, Y. Ding, and R. Velraj, "Role of PCM addition on stratification behaviour in a thermal storage tank – An experimental study," *Energy*, vol. 115, pp. 1168–1178, 2016.
- [89] J. Fan and S. Furbo, "Thermal stratification in a hot water tank established by heat loss from the tank," *Sol. Energy*, vol. 86, no. 11, pp. 3460–3469, Nov. 2012.
- [90] Z. Lavan and J. Thompson, "Stratified Hot Water Storage Tanks," *Small*, vol. 19, pp. 519–524, 1976.
- [91] A. Elatar, K. Nawaz, B. Shen, V. Baxter, and O. Abdelaziz, "Characterization of Wrapped Coil Tank Water Heater During Charging/Discharging," in *ASME Proceedings Paper*, 2018, pp. 1–8.
- [92] J. D. Rendall, F. Karg Bulnes, Kyle R. Gluesenkamp, A. Abu-Heiba, W. Worek, and K. Nawaz, "A Flow Rate Dependent 1D Model for Thermally Stratified Hot-Water Energy Storage," *Energies*, vol. 14, no. 2611, 2021.
- [93] G. H. Jirka, "Integral Model for Turbulent Buoyant Jets in Unbounded Stratified Flows Part 2: Plane Jet Dynamics Resulting from Multiport Diffuser Jets," *Environ. Fluid Mech.*, vol. 6, no. 1, pp. 43–100, Jan. 2006.
- [94] W. E. Frick, "Non-empirical closure of the plume equations," *Atmos. Environ.*, vol. 18, no. 4, pp. 653–662, 1984.
- [95] R. W. Mott and A. W. Woods, "On the mixing of a confined stratified fluid by a turbulent buoyant plume," *J. Fluid Mech.*, vol. 623, pp. 149–165, 2009.
- [96] A. A. Grachev, E. L. Andreas, C. W. Fairall, P. S. Guest, and P. O. G. Persson, "The Critical Richardson Number and Limits of Applicability of Local Similarity Theory in the Stable Boundary Layer," *Boundary-Layer Meteorol.*, vol. 147, no. 1, pp. 51–82, Apr. 2013.
- [97] S. Kumar, R. B. Grover, H. Yadav, P. K. Vijayan, U. Kannan, and A. Agrawal, "Experimental and numerical investigation on suppression of thermal stratification in a water-pool: PIV measurements and CFD simulations," *Appl. Therm. Eng.*, vol. 138, pp. 686–704, Jun. 2018.
- [98] W. D. Smyth and J. N. Moum, "Length scales of turbulence in stably stratified mixing layers," *Phys. Fluids*, vol. 12, no. 6, pp. 1327–1342, 2000.
- [99] D. A. Briggs, J. H. Ferziger, J. R. Koseff, and S. G. Monismith, "Turbulent mixing in a shear-free stably stratified two-layer fluid," *J. Fluid Mech.*, vol. 354, pp. 175–208, Jan. 1998.
- [100] A. M. Obukhov, "Turbulence in an atmosphere with a non-uniform temperature," *Boundary-Layer Meteorol.*, vol. 2, no. 1, pp. 7–29, 1971.
- [101] C. Shi and P. Hrnjak, "Effect of the Use Pattern on Performance of Heat Pump Water Heater," in *17th International Refrigeration and Air Condition Conference at Purdue*, 2018, p. 2303.